Supplemental information for the paper

From shrimp balls to hydrogen bubbles: Borohydride hydrolysis catalysed by flexible cobalt chitosan spheres

Frances Pope [a], Jeffrey Jonk [a], Millie Fowler [a], Petrus C. M. Laan [a], Norbert J. Geels [a], Larissa Drangai [b], Vitaly Gitis [c] and Gadi Rothenberg *[a]

---

[a] Van 't Hoff Institute for Molecular Sciences, University of Amsterdam, Science Park 904, Amsterdam 1098 XH, The Netherlands. Email: g.rothenberg@uva.nl

[b] Austrian Centre of Competence for Tribology, AC2T research GmbH, Viktor-Kaplan-Straße 2, Wiener Neustadt, 2700, Austria

[c] Faculty of Engineering Sciences, Ben-Gurion University of the Negev, PO Box 653, Beer-Sheva 8410501, Israel

Additional analysis data (figures S1–S10): XPS of the chitosan spheres, adsorption isotherms, high-precision kinetics experiments and the resulting Arrhenius plots, TOF vs temperature analysis, additional reaction profiles, UV-Vis of used fuel.

Detailed experimental procedures and descriptions, schematics and photos of the batch reactor setup and the continuous reactor setup used in the experiments (schemes S1 and S2 and figures S11 and S12).

Table S1. Stability and longevity of catalysts for borohydride hydrolysis. *Time calculated from reusability tests

Catalyst	Reactant	Reactant conc.	Hydroxide	Number of batch runs	Longest catalyst exposure time (mins)	Ref
Co chitosan spheres	KBH_4	5 %	5 % KOH	5	2,880	This work
Co/γ-Al2O3	KBH_4	5 %	5 % KOH	1	1,200	This work
Co/θ-Al2O3	KBH_4	5 %	5 % KOH	1	960	This work
Co/MgO	KBH_4	5 %	5 % KOH	1	300	This work
Co-B/AC	KBH_4	5 wt%	1 wt% NaOH	1	35	[1]
Ni-Mo-Ru–B@TiO_2	KBH_4	2.5 w/w%	6 % KOH	1	30	[2]
Pd/C	$NaBH_4$	2.95 mmol	To pH 13	1	125	[3]
Pd/$CoFe_2O_4$	$NaBH_4$	1 mmol	None	5	12	[4]
PtNi/PTOC	$NaBH_4$	1.5 wt%	5 wt% NaOH	8	25	[5]
MoS_2/POAC	$NaBH_4$	1 %	None	11	165*	[6]
NiAc@PVDF-HFP MNFs	$NaBH_4$	2.67 mmol	Alkaline	10	600	[7]
RuW/MWCNT	$NaBH_4$	0.26 M	None	5	55	[8]
CoB-zeolite-HCl	$NaBH_4$	5 %	1 % NaOH	4	200	[9]
$CoFe_2O_4$@N,S-G	$NaBH_4$	1 M	NaOH pH 10 added	1	7	[10]
Co/MWCNTs-20	$NaBH_4$	n/a	None	5	100*	[11]
Co_3O_4/SiO_2	$NaBH_4$	5 %	5 % NaOH	1	7	[12]
CNSs@Co	$NaBH_4$	0.25 M	0.25 M NaOH	5	30	[13]

CoB/Ag-TiO_2	$NaBH_4$	1 wt%	5 wt% NaOH	5	40	[14]
Co@C-700	$NaBH_4$	2 wt%	2 wt% NaOH	5	300	[15]

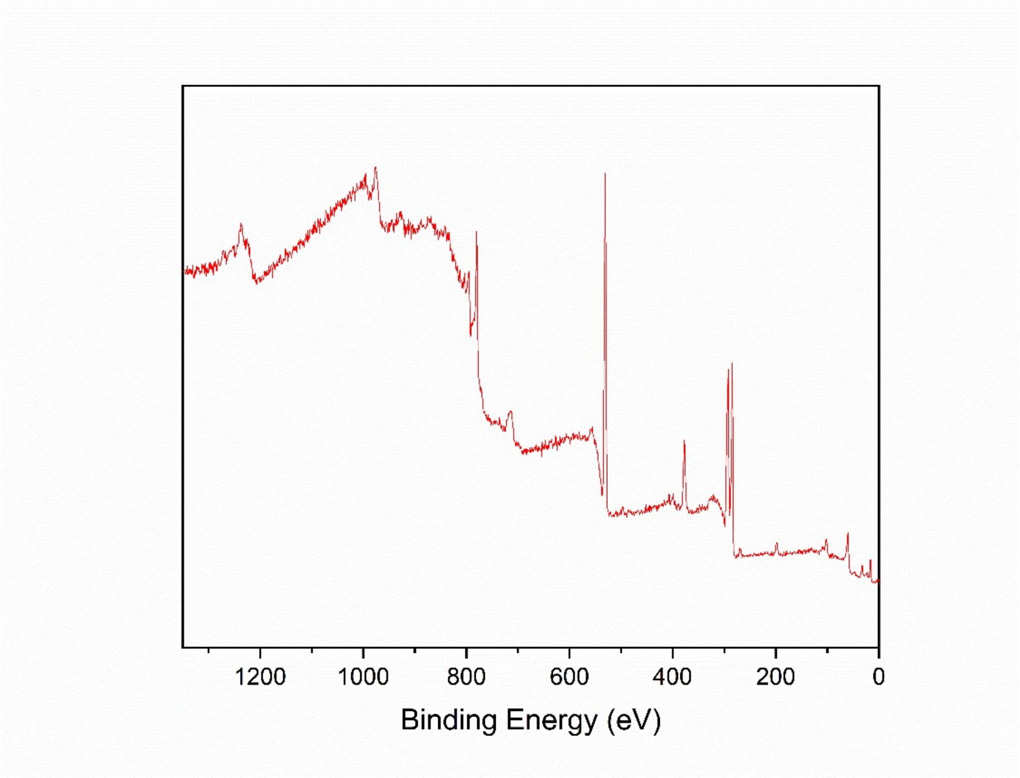

Figure S1. XPS survey spectrum of a pristine cobalt chitosan sphere.

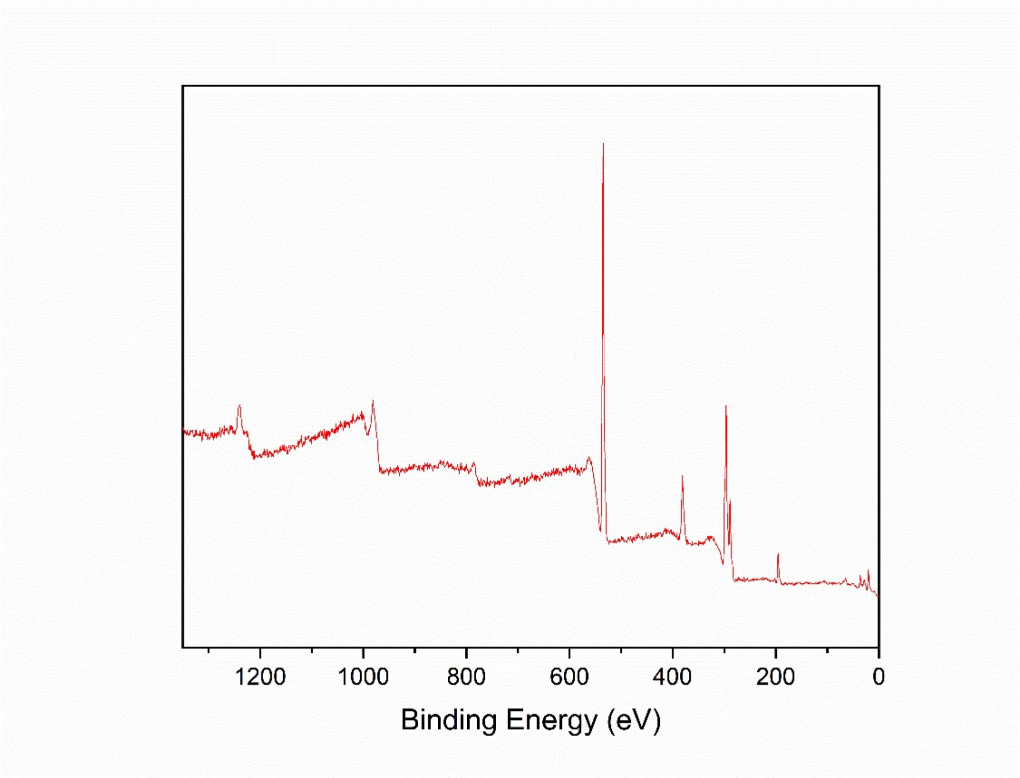

Figure S2. XPS survey spectrum of used cobalt chitosan sphere.

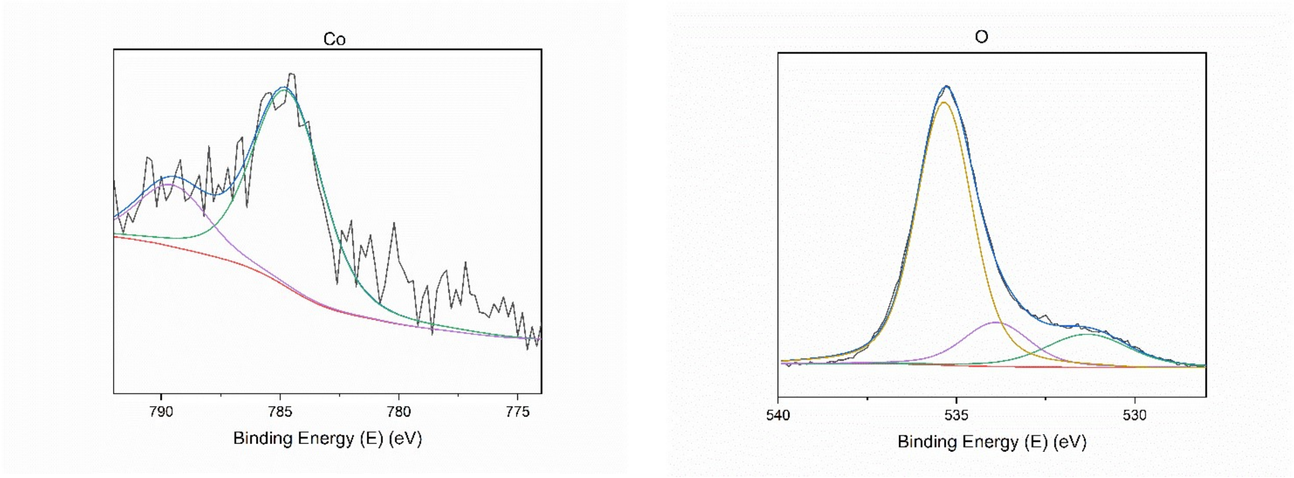

Figure S3. XPS results for the cobalt chitosan sphere after multiple runs – Co 2p (a) and O 1s (b).

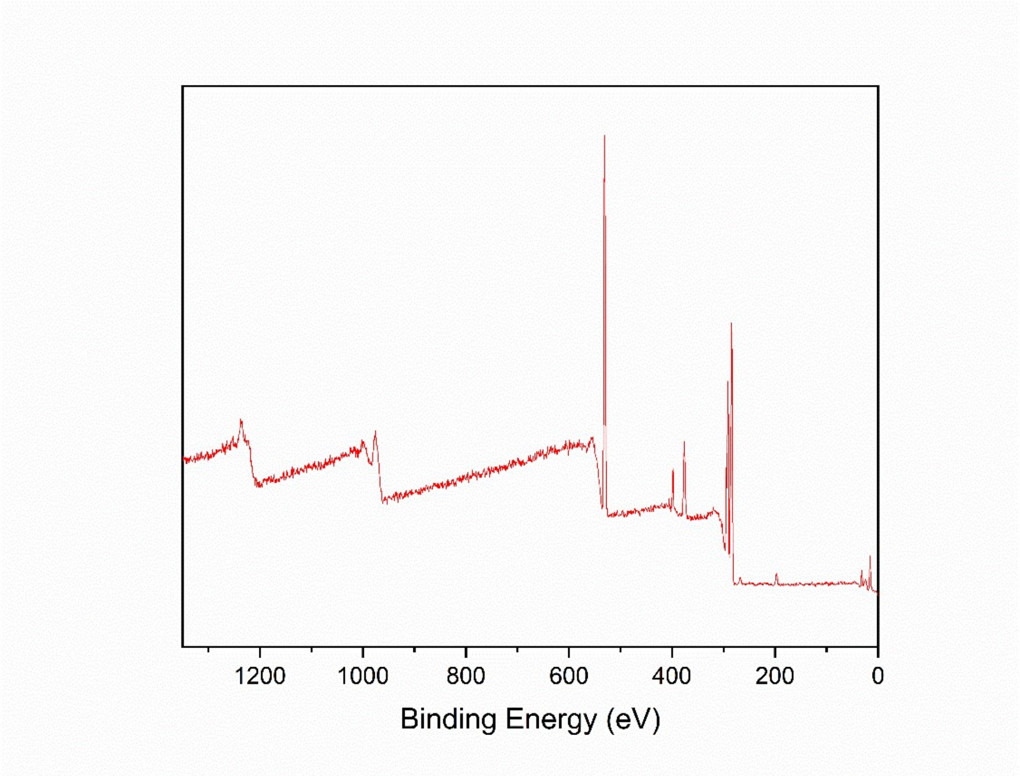

Figure S4. XPS survey spectrum of blank chitosan sphere.

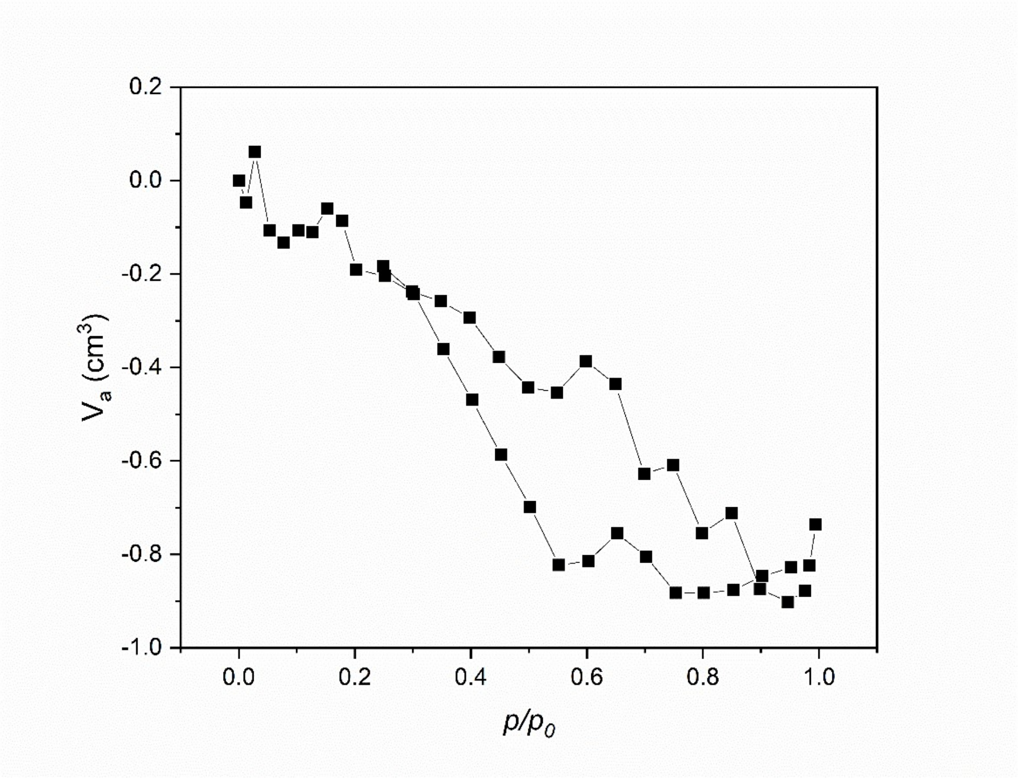

Figure S5. Nitrogen adsorption isotherm at 77K of cobalt chitosan spheres pre-treated at 70 °C.

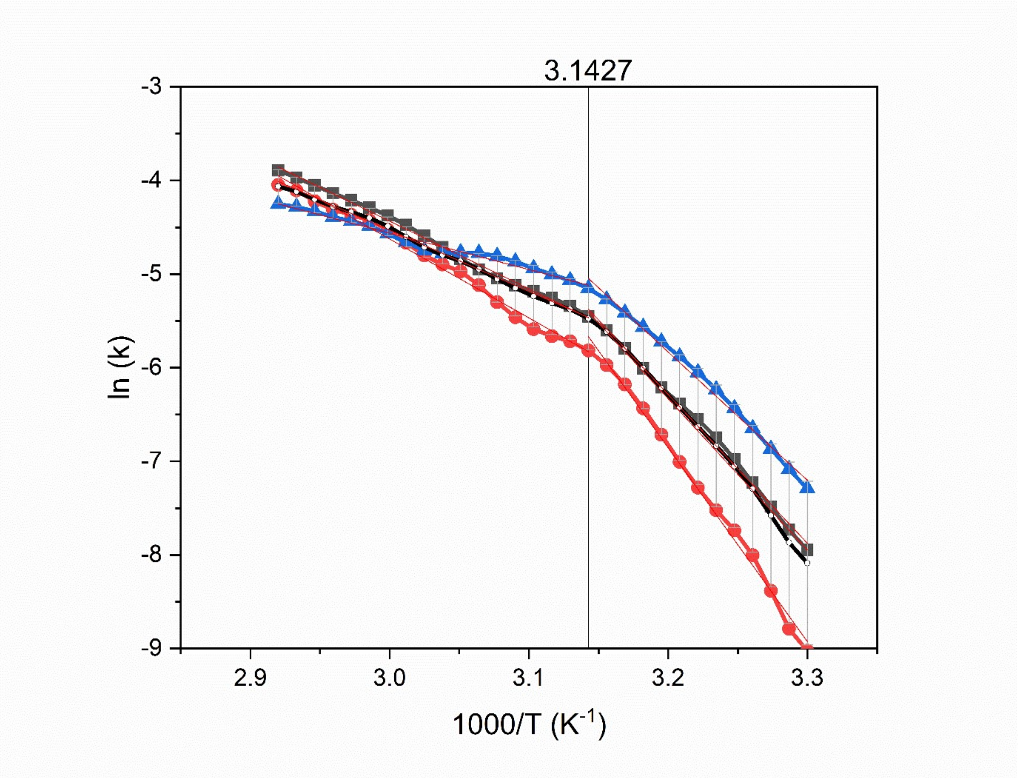

Figure S6. Three measured sets of Arrhenius data in blue (triangles), grey (squares) and red (circles). Average in black with error bars. 3.1427 marks the centre of the 'kink' seen throughout the measurements, as explained in the main text.

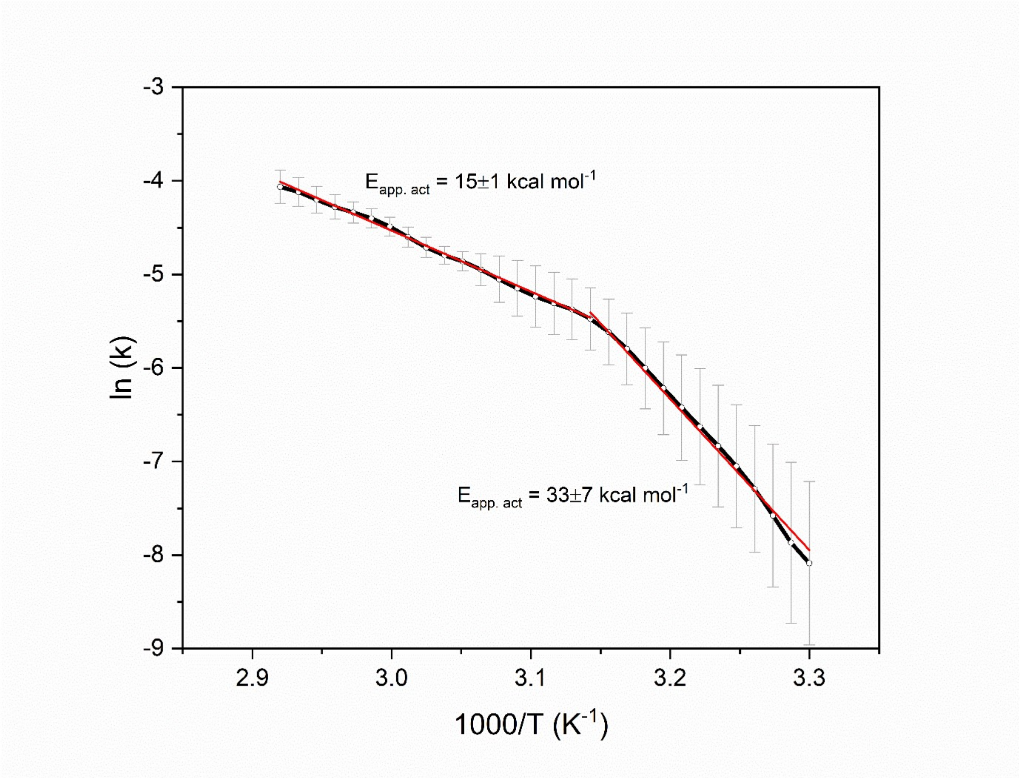

Figure S7. The average of all three sets of Arrhenius plot measurements (in black) with error bars. Red linear fit lines show where the E_A was calculated.

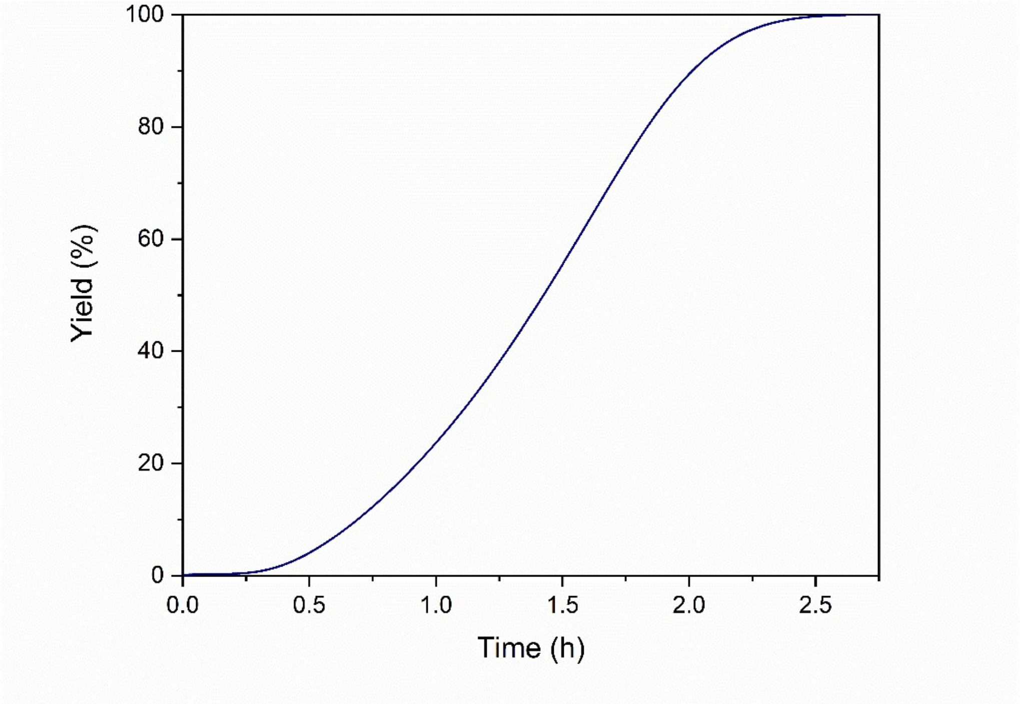

Figure S8. Cobalt chitosan spheres (0.25 g) in fuel (5 w/w% KBH_4, 5 w/w% KOH in H_2O, 15 mL) at 40 °C. Measurements taken by mass flow meters every second.

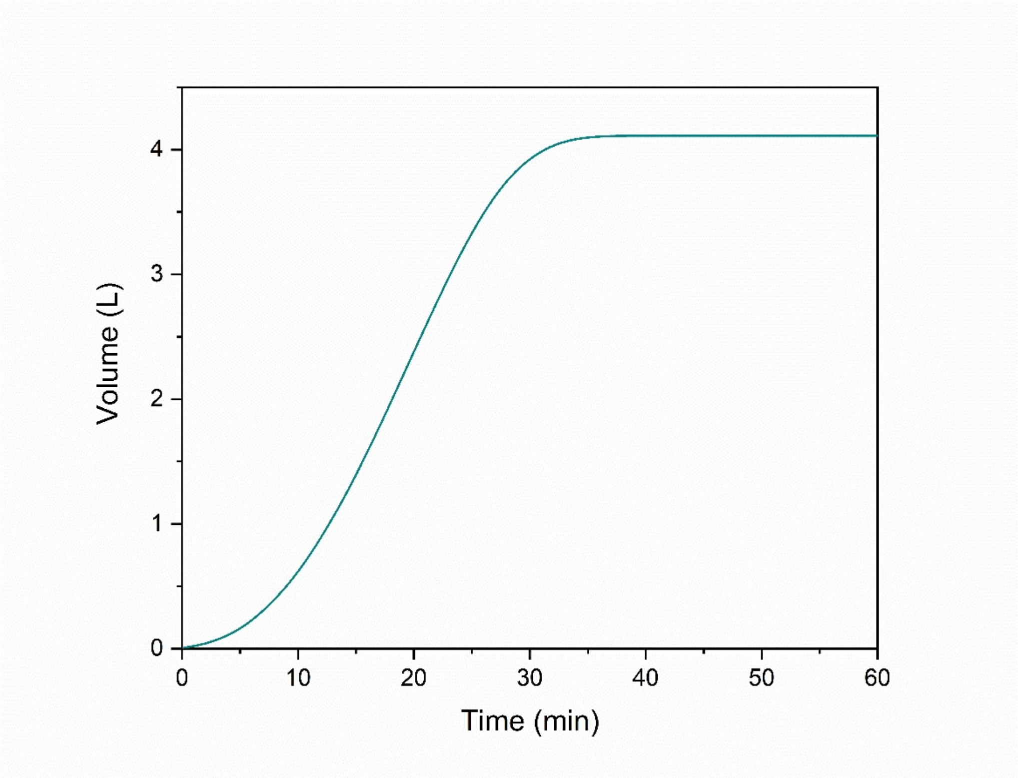

Figure S9. Cobalt chitosan spheres (0.25 g) in $NaBH_4$ fuel (molar equivalent to KBH_4 fuel (50 mL) at 65 °C. Measurements taken by mass flow meters every second.

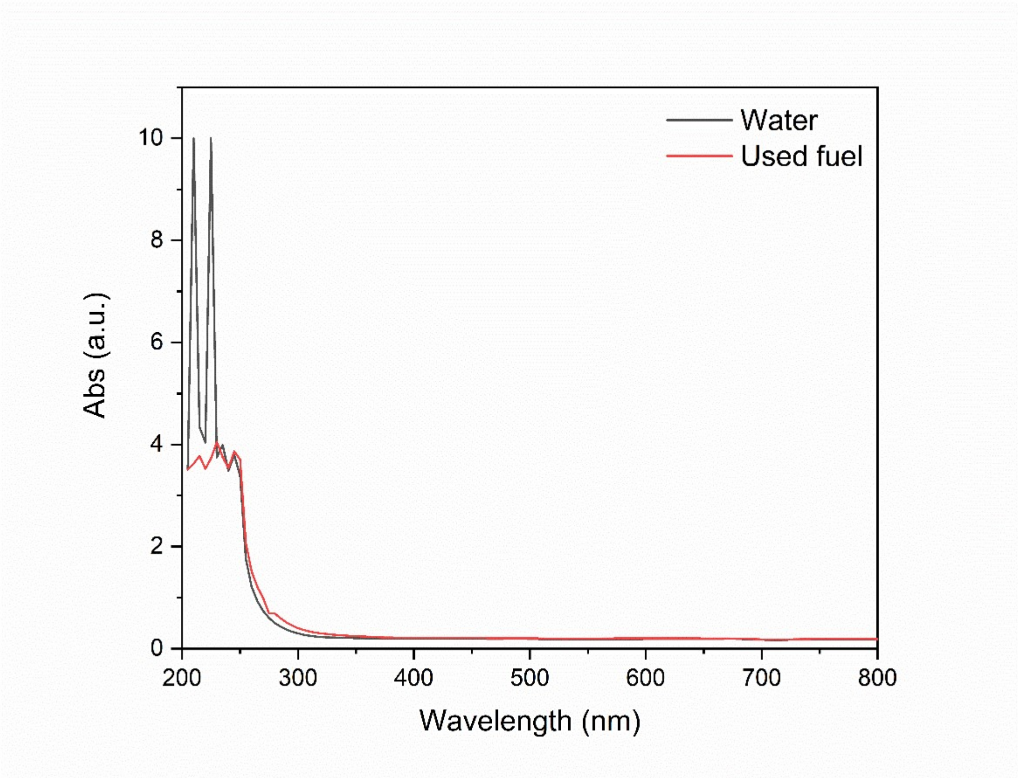

Figure S10. UV-Vis spectrum of used fuel vs water. After an experiment with the catalyst, the spheres were filtered and UV-Vis of the used fuel was taken. No soluble species were seen.

Experimental methods

Al_2O_3 and MgO- Al_2O_3 (ESM 350E) and MgO were sourced from Albemarle (formerly Ketjen) Eurosupport and Strem Chemicals, respectively.

Blank chitosan ball synthesis. Metal-free chitosan balls were synthesised as “blanks” to confirm that the cobalt was the source of catalysis of KBH_4.

In one beaker, chitosan is mixed with acetic acid in a beaker until a homogeneous gel solution is formed. Then, in a separate beaker, a solution with HCl was made (without any metal salt). These were both mixed together homogeneously and then extruded through a syringe and needle into a 4 M KOH solution. The balls were collected by filtration and left to dry in air. This resulted in clear, small and gelatinous balls which were tested in borohydride solution.

Low temperature reaction. A reaction was also done at lower temperatures (below the ‘kink’ point in the Arrhenius plot) to confirm that the chemical mechanism of the reaction did not differ from that at higher temperatures. This reaction was done in the batch reactor. (See Figure S9).

Al_2O_3 and MgO supported Co catalysts. γ-Al_2O_3 was bought as extrudates. θ-Al_2O_3 was prepared from γ-Al_2O_3 by heat treatment. MgO was bought as powder and pressed into pellets using a pellet press. γ- Al_2O_3 was put in a furnace set to 1050 °C for 3 h in air (ramp rate of 5°C/min). This gives a mixture of δ-Al_2O_3 and θ-Al_2O_3. Note that heating the γ-Al_2O_3 at 1050 °C but for 5 h with a slower ramp rate (2°C/min) results in predominantly α-Al_2O_3 formation. MgO was dry-pressed into 50x10 mm cylindrical coupons and sintered at 1000 °C for 4 h. All three supports were impregnated by the same method.

$Co(NO_3)_2{\cdot}6H_2O$ (1 M) was dissolved in H_2O. This was then added to the extrudates at a ratio of 0.5 mL of solution per gram of support. The mixture was shaken for 5 min to ensure homogeneity. It was then left at room temperature for 3 h, shaken occasionally. The extrudates were then dried in air at 110 °C for 8 h and subsequently calcined in a furnace in air at 450 °C for 2 h (ramp rate of 5°C/min). This resulted in a 7 wt% Co supported catalyst. This was done for γ-Al_2O_3, θ-Al_2O_3 and MgO.

Reactor Setups

Batch reactor setup. The batch reactor setup remained constant throughout all experiments. A 100 mL three-neck round-bottom flask containing a stir bar is placed in a silicon oil bath. The oil bath is preheated to 65 °C. To close the system, a 50 mL dropping funnel is places in one neck. The top of the dropping funnel is sealed with a tap and an injection point to flush the system with air. The middle neck is closed with a septum. The last neck is connected to a cold trap for H_2 to flow out of the reactor. All glass-glass connections are sealed with silicon grease and clipped in place. The cold trap is cooled on ice water. Ice is topped up regularly to ensure total cooling. Two mass flow meters are connected to the cold trap output in series: firstly with a maximum of 200 mL_n/min, then with a maximum of 2 L_n/min. The rate of gas flow is measured in both MFMs every second and logged in an excel file. All joints within the system are checked regularly for leaks using a hydrogen leak detector, which measures in ppm. All reactions recorded showed no leaks in the setup.

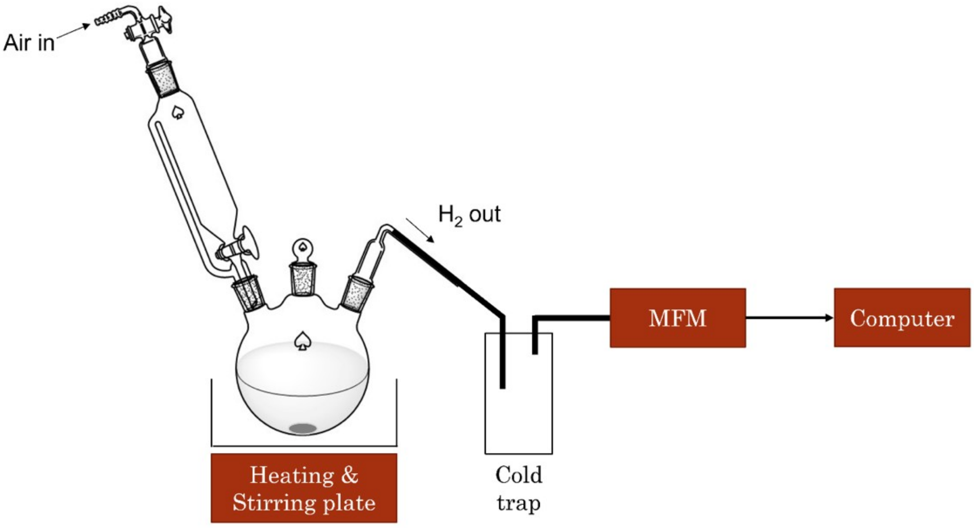

Scheme S1. Schematic of batch reactor setup during experiment

Before an experiment, the silicon oil bath is preheated and the catalyst, KBH_4 and stir bar put in the RBF. KOH is dissolved in H_2O and preheated to 5 °C above the reaction temperature. This is to take into account the cooling that will occur during setup of the reaction as well as flushing with air before the reaction starts. The setup is put together and flushed with air three times, then the gas tap at the top of the dropping funnel is cl ng plate is set to 120 rpm. Once the flow rate has returned to ze into the RBF and data collection from the MFMs starts. The data omplete.

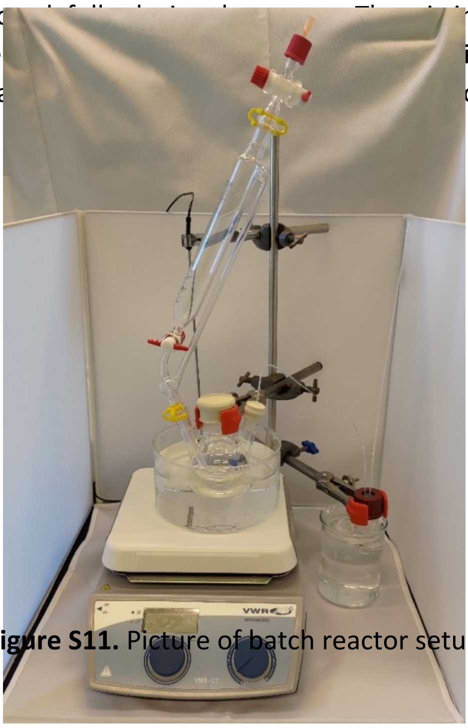

Figure S11. Picture of batch reactor setup

Continuous reactor setup. Catalyst was added to the central reactor column and held in place with an O-ring, stainless steel mesh and protected with quartz wool. This was to stop any broken catalyst particles from passing through the reactor lines into the waste line. This was set up in the oven and tightened with Swagelok connections and O-rings. The oven was then heated to 65 °C with heat circulation by a fan.

Fuel for the continuous reactor was made in batches of up to 1 L and added to the fuel tank. KOH (50 g, 0.9 mol, 5 w/w%) was dissolved in H_2O at room temperature. Then, KBH_4 (50 g, 0.9 mol, 5 w/w%) was dissolved in the solution. This was added to the fuel tank and fed into the continuous reactor by a liquid pump. The liquid was pumped at a high rate until it reached the bottom of the reactor tube. Then, the slow pump rate of 0.8 mL/min was set. Once it reached the catalyst, the flow meters were started. The gas flows through a separator, a gas bubbler containing water and then two mass flow meters in series. The first at a low flow rate of up to 200 mL_n/min, then a high flow rate of up to 2 L_n/min. All waste liquid drops from the separator down a line to the waste bin. The solution should have cooled to room temperate, be stabilised and separated from any catalyst, so H_2 from waste should be negligible.

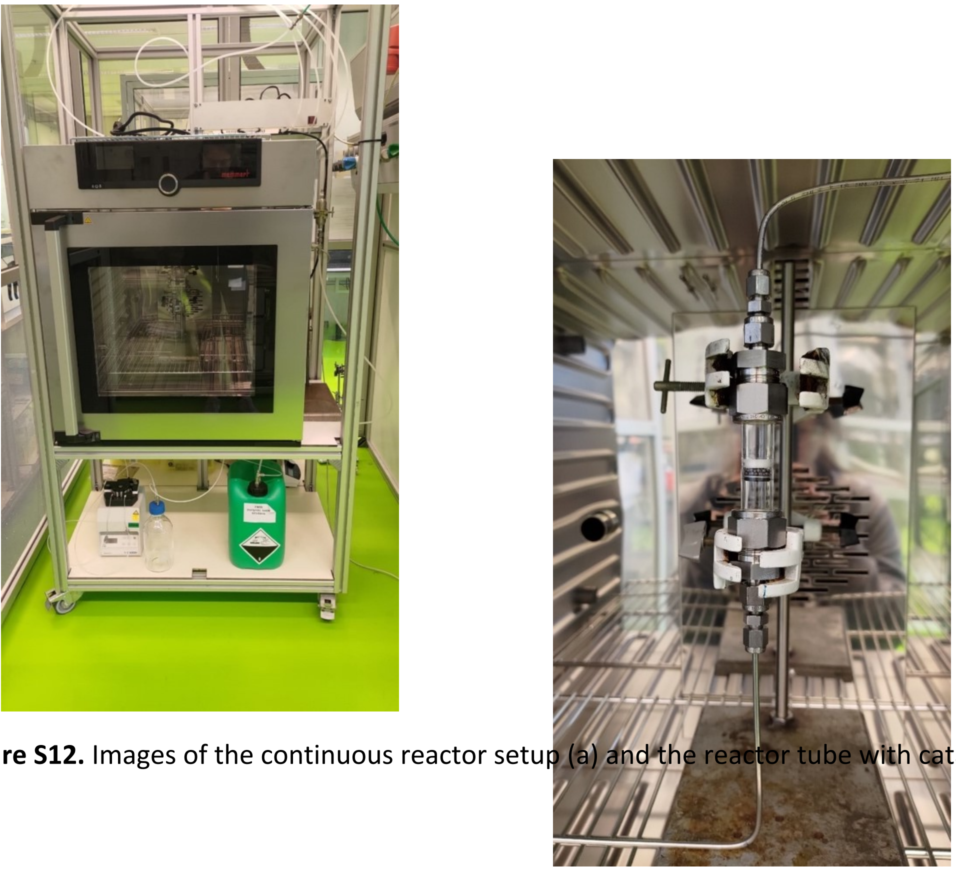

Figure S12. Images of the continuous reactor setup (a) and the reactor tube with catalyst bed (b)

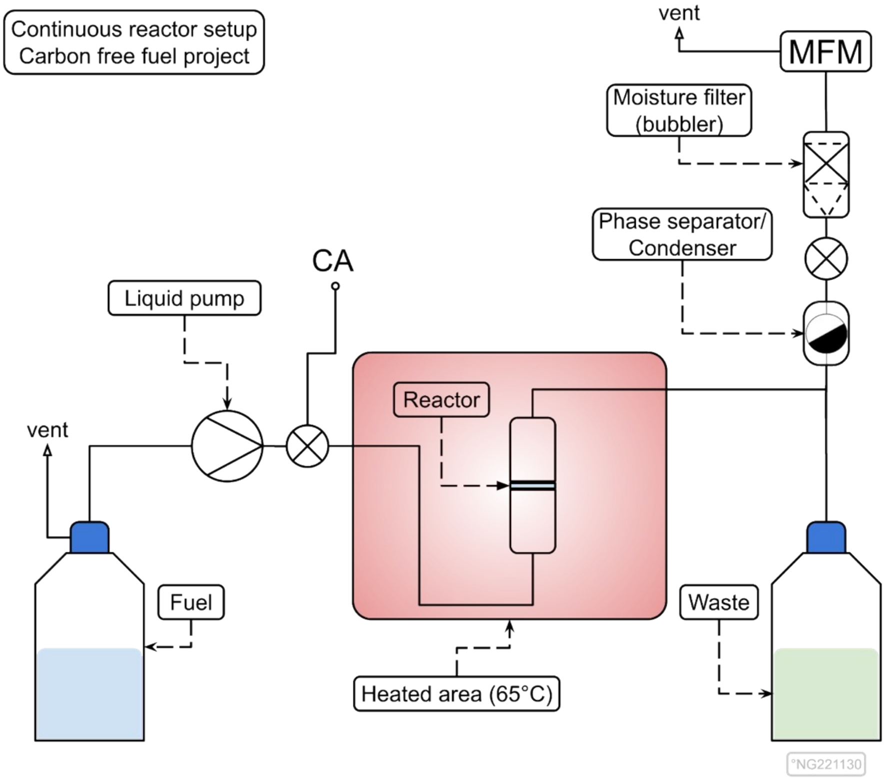

Scheme S2. Schematic of continous reactor system.

References

[1] D. Xu, H. Wang, Q. Guo, S. Ji, *Fuel Process. Technol.* **2011**, *92*, 1606–1610.

[2] M. Salih Keskin, Ö. Şahin, S. Horoz, *J. Aust. Ceram. Soc.* **2022**, DOI 10.1007/s41779-022-00755-w.

[3] N. Patel, B. Patton, C. Zanchetta, R. Fernandes, G. Guella, A. Kale, A. Miotello, *Int. J. Hydrog. Energy* **2008**, *33*, 287–292.

[4] Y. Wang, X. Liu, *ACS Appl. Nano Mater.* **2021**, *4*, 11312–11320.

[5] Y. Yu, L. Kang, L. Sun, F. Xu, H. Pan, Z. Sang, C. Zhang, X. Jia, Q. Sui, Y. Bu, D. Cai, Y. Xia, K. Zhang, B. Li, *Nanomaterials* **2022**, *12*, 2550.

[6] K. Rambabu, A. Hai, G. Bharath, F. Banat, P. L. show, *Int. J. Hydrog. Energy* **2019**, *44*, 14406–14415.

[7] A. M. Al-Enizi, M. M. El-Halwany, S. F. Shaikh, B. Pandit, A. Yousef, *Arab. J. Chem.* **2022**, *15*, 104207.

[8] T. Avcı Hansu, *Int. J. Hydrog. Energy* **2023**, *48*, 6788–6797.

[9] C. Saka, M. Salih Eygi, A. Balbay, *Int. J. Hydrog. Energy* **2020**, *45*, 15086–15099.

[10] H. Jafarzadeh, C. Karaman, A. Güngör, O. Karaman, P.-L. Show, P. Sami, A. A. Mehrizi, *Chem. Eng. Res. Des.* **2022**, *183*, 557–566.

[11] K. Narasimharao, B. M. Abu-Zied, S. Y. Alfaifi, *Int. J. Hydrog. Energy* **2021**, *46*, 6404–6418.

[12] P. K. Singh, T. Das, *React. Kinet. Mech. Catal.* **2021**, *134*, 677–696.

[13] H. Zhang, G. Xu, L. Zhang, W. Wang, W. Miao, K. Chen, L. Cheng, Y. Li, S. Han, *Renew. Energy* **2020**, *162*, 345–354.

[14] X. Shen, Q. Wang, Q. Wu, S. Guo, Z. Zhang, Z. Sun, B. Liu, Z. Wang, B. Zhao, W. Ding, *Energy* **2015**, *90*, 464–474.

[15] X. Zhang, X. Sun, D. Xu, X. Tao, P. Dai, Q. Guo, X. Liu, *Appl. Surf. Sci.* **2019**, *469*, 764–769.